



TRANS QUASI Z-SOURCE INVERTER POWERED WIND SYSTEM WITH AN INCREASING VOLTAGE PROFILE

RAJENDRAN ELUMALAI¹, RAJI VARADHAN²

Keywords: Permanent magnet synchronous generator (PMSG); Trans-quasi-Z-source inverter (Trans-QZSI); Space vector pulse width modulation (SVPWM); Total harmonics distortion (THD); Z-source inverter (ZSI).

The majority of the world's future energy contribution is expected to come from renewable energy sources. The current power system has numerous nonlinear load demands and relies on a power electronics converter, resulting in significant power quality issues. In this study, the space vector pulse-width modulation (SV-PWM) technique is employed to control the trans-quasi z-source inverter (Trans-QZSI) powered by permanent magnet synchronous generators (PMSG), thereby enhancing the power quality of wind energy systems. Additionally, the PMSG is small and has a low volume, which is a unique characteristic. This leads to a closed-loop regulator's objective of efficiently controlling a three-phase contribution of steady voltage through the use of a trans-QZSI. By increasing the input DC voltage, the inductor will provide a higher output DC voltage. Due to the shoot-through mode, the DC utilization voltage of the Z-source network will increase. The shoot-through task ratio is controlled by the closed-loop checker, which also closely monitors the principal variable voltage. Because it provides a synchronised three-phase output voltage, the intended closed-loop architecture is a strong choice for both boosting and essential dynamic and secure state management. Here, the inverter is managed using the space vector PWM approach. From the simulation point of view, the suggested total harmonic distortion (THD) was 0.032%; however, from the experimental point of view, THD was 2.093%.

1. INTRODUCTION

The present decade has seen wind energy play a significant role in the global power production system. Particularly, Induction Generators (IGs) with Doubly Fed Induction Generators (DFIGs) are utilized effectively. A predictable IG stator is directly attached to the grid; additionally, the rotor is a closed ring coil. The stator side is only connected to the grid network. When utilized, IGs and DFIGs are additionally mandatory in the grid power [1,2]. Because these generators initially run at a speed below their rated speed, this mode is referred to as motor mode, resulting in the absorption of reactive power by the grid. Suppose these generators are run at a speed above their rated speed, which supplies the reactive power to the grid, also known as generator mode. A supplementary present with an additional flexible description of the IG utilizing massive wind turbines is an alternative called DFIG. Conversely, the DFIG rotor has three-phase windings that connect to the grid through power electronic converters. Here, converters permit magnetic fields of rotor windings to interact through the magnetic field within stator windings, making a torque [3]—this torque's potency of the two fields as well as the phase angle between them.

Also possible for wind turbines is working with the overprotective at a range of rotating rates, achieving about $\pm 30\%$ of the grid frequency. Power converters are permitted to operate back-to-back at the remaining frequencies. These are all the problems with the DFIG and IG systems [4-5]. In the present year, it is mainly utilized as a PMSG. Because there is no need for grid power to begin power production, less volume and weight are also special characteristics, and all these are the benefits of PMSG [6]. This study discusses the PMSG control approach for a small wind turbine located in a remote area. The sliding mode control (SMC) approach has gained popularity in recent years.

Furthermore, the PI controller is a linear regulator, which is not suitable for wind turbines since the system exhibits nonlinear behaviour in both its electrical and mechanical components [7]. There are several similarities between the PMSG control utilised in induction machines and mentoring applications. Feedback linearisation control (FLC) can be utilised to find the optimal solution in the

current paper due to the nonlinearity of wind energy conversion systems (WECS). In this instance, the control technique is developed from the partially linearized model, and the findings obtained allow for exact linearization [8]. This article looks at the DFIG as well as PMSG distress voltage constancy. The voltage permanence of WECS is supported by PMSG, as well as DFIG, in three separate developments. The entire arrangement is also designed to facilitate the smooth progress of MATLAB. Results of this investigation include extensive consequences [9].

This mission suggested an improved Z-source inverter topology. Evaluated usual ZSI is high voltage stress expansively to build the analogous voltage boost, as well as restriction to inrush current by start-up. The managed approach of the proposed trans-QZSI is like a conventional one; every live control strategy is employed honestly. The soft-start approach is planned to restrain the inrush current; moreover, the significance of Z-source capacitors and inductors is also considered. This procedure's attitude toward the planned technology, moreover, will be evaluated in detail within the usual topology [10].

This paper presents the digital implementation of SVPWM, supporting various switching progressions of ZSI. The innovation of manuscript plans with every switching evolution allows a state of balance; moreover, the functioning of complex bus clamping methods of ZSIs [11]. The Trans QZSI, through its improved buck-boost potential, surpasses every reward of the fixed ZSI; moreover, it alters the conventional voltage source inverter PWM. This paper presents work on third harmonic injection, as well as maximum constant boost control, a technique that has been widely used [12]. This article aims to utilize the PI checker GWO algorithm for an enhanced and confident display of DPFC. Consequently, power quality worsens severely, and similar time harmonics are also concentrated at a remarkable stage of 4.62% of voltage THD. This article also employs the same SVPWM techniques as the proposed method, resulting in a low total harmonic distortion (THD) level [13]. This study introduces a fresh artificial intelligence method called convolutional neural network (CNN). An AI method is planned in this scheme to improve power quality due to instability significantly. This move is towards well-dealing with

¹ SKP Engineering College, Tiruvannamalai, Tamil Nadu, India. E-mails: rajendran_electro@skpec.in. raji.vpm@skpec.in

reactive power reparation, moreover, previous current connected power quality problems, plus harmonics. This post prepares the MATLAB simulation; the hardware portion is not included [14]. This study presents an ESOA-supported FCS-MPC method (ESOA FCS-MPC) with DPFC to address power quality concerns in HRES schemes by handling both real and reactive power. Supporting the simulation model outcome, DPFC maintains the feature of power; moreover, it decreases the THD current and voltage by 0.86% and 0.49%, respectively. However, the hardware part results are not the primary focus of this document [15]. This article via ASB-qZSI, the shoot-through function relation reduces modulation trouble. Subsequently, the projected move towards the MATLAB software has also been a success, as observed through active performances, with the hardware part not discussed [16]. This effort is part of a widespread scheme that connects ripple-open quasi-Z-source (QZS) converter systems, as well as integrates an improved power supervision scheme, including a controlled storage battery linked bidirectional buck-boost converter. A PI controller implements the battery charge and discharge process to maximise the battery's stored energy. System standalone operation is implemented, resulting in overall efficiency reduction, and it is not possible to obtain the experimental part [17].

This point suggests a double space vector rule approach, quasi-Z-source direct matrix converter (QZSDMC) is a prepared quasi-Z-source network attached matrix converter (MC). Subsequently, a double space vector PWM method for QZSDMC analyzed the sharing of shoot-through occasions during zero vectors. It is not appropriate to address this paper in THD level analysis [18]. This document presents an innovative process to identify and categorize PQ instability based on a customized Stockwell Transform (ST) source of report, as well as Hybrid Grey Wolf Optimization (HGWO) for quality collection through K nearest neighbour (KNN) classifier. MATLAB is approved for a broad range of eighteen copied PQ measures to certify the value of a certain description.

Additionally, a trial is extensive for six modules of actual PQ dealings obtained from a self-excited induction generator (SEIG) structure during a laboratory trial group. Compared to PMSG functionality, SCIG is less complex, resulting in a more straightforward system operation [19]. Therefore, the central offerings of this object include a clear description, restrictions of the DCM, as well as the growth of small-signal representation to facilitate acquiring a keen understanding of the dynamics of the exacting Z network controlled via the trans-QZSI converter, which authorizes the performance of the system operational in DCM, as examined below, in the altered current requirement situation. However, harmonic analysis was not covered in this document [20]. According to the poll, PMSG is the more effective way to improve power quality, while Trans-QZSI primarily raised the voltage profile. Thus, the primary goal of this paper

- To ensure the smooth operation of the financial utilization of the inverter controlled by SVPWM.
- To provide the most favourable wind energy generation, moreover, improved dynamic performances compared to the conventional method.
- To reduce THD and provide a constant supply voltage to the three-phase grid using an SVPWM controller.

- To implement MATLAB simulation and experimental models. Reduce the task cycle when the converter is working in the shoot-through mode.

2. MATERIALS AND METHODOLOGY

Fig.1 shows that PMSG is integrated with the trans-QZSI through the wind energy system. Initially, the wind speed and the wind turbine can rotate. Based on the wind turbine speed, PMSG can produce 3-phase AC power. AC power is provided to the diode rectifier circuit. This network changes the AC power near DC power; as a result, DC power is supplied to the trans-QZSI circuit. Here, Trans-QZSI applies the shoot-through mode; now, the DC side is boosted. The enhanced DC power is provided to the inverter. Further, the DC power is converted to AC, and this AC power is supplied to the LC filter and transformer circuit. The transformer matches the grid frequency, and the LC filter performs the primary function and removes harmonic content from the inverter output. In addition, the grid real and reactive power are compared to the SVPWM network. Based on the error signal, SVPWM produces the PWM signal. Based on the PWM signal, the inverter can supply grid power.

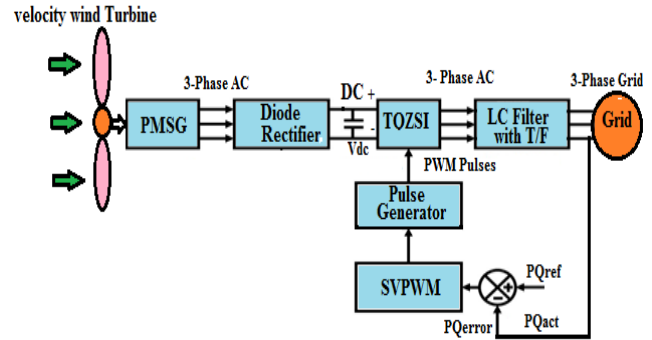


Fig. 1 – Proposed simulation block diagram.

2.1 TRANS-QZSI ANALYSIS

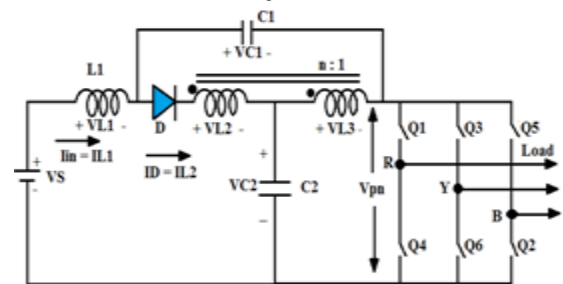


Fig. 2 – Trans-QZSI.

The planned trans-QZSI is enhanced and evaluated compared to the conventional trans-Z Source Inverter. The proposed circuit, a single inductor in addition to a diode, is shown in Fig. 2. Like the previous Z-Source Inverter skill, shoot-through mode zero states are included in the two usual zero states modes of the proposed inverter. Therefore, excluding the inverter from the standard process of the proposed inverter enhances the buck-boost role. The corresponding Trans-QZSI operating in shoot-through mode is illustrated in Fig. 3, where the key voltage, V_s , is specified near capacitor C_1 and inductor L_1 . Trans-QZSI is shorted; moreover, diode D is off. Capacitor C_2 recharges through inductor L_3 , and the magnetization current of the

inductor is amplified gradually. Since L2 and L3 inductors are attached securely, the excitation currents are reflected into the secondary windings of the joined inductor. Voltage increases L2 from a bit of value to VL2 equal to nVL3, and the L2 inductor is charged. Further, the voltage of the L2 inductor is high, as well as the diode holding out the reverse power. Now, the shoot-through duty ratio D is expressed,

$$T_o = DT \quad (1)$$

$$T_s = (1 - D)T \quad (2)$$

$$VL3 = VC2 \quad (3)$$

$$VL2 = nVL3 = nVC2 \quad (4)$$

$$VL1 = V_s + VC1 \quad (5)$$

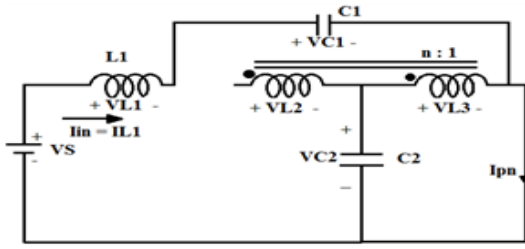


Fig. 3 - Shoot through mode.

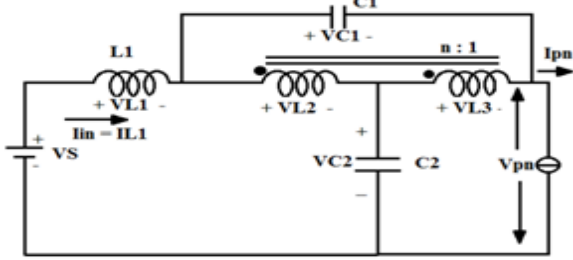


Fig. 4 - Non-shoot-through mode.

The corresponding Trans-QZSI operated on the non-shoot-through mode is exposed Fig. 4. T-shoot-e D is on Trans-QZSI forced through current source. The pairing of inductors L2 and L3, as well as the contribution of inductor L1's power to the load, occurs mutually. Additionally, the capacitor is provided with voltage, resulting in an enhanced trans-QZSI.

$$-VC1 = VL2 + VL3 \quad (6)$$

$$VL1 = V_s - VL2 - VC2 \quad (7)$$

$$V_{pn} = VC2 - VL3 \quad (8)$$

Since the beyond investigation trans-QZSI is controlled through diode D. Shoot-through state and non-shoot-through state conditions, to transmit the energy accumulated in the pairing inductor with contribution inductor just before attaining the enhanced function. In support of inductors L1, L2, L3, the standard voltage available at the same time switching stage is zero.

$$\frac{1}{T} \left[\int_{t_o}^{t_1} VL dt + \int_{t_1}^{t_2} VL dt \right] = 0 \quad (9)$$

From the over scrutiny, moreover, supported on the "Volt-Second" equilibrium relation

$$DVC2 - (1 - D)(VC1 + VL2) = 0 \quad (10)$$

$$nDVC2 - (1 - D)(VC1 + VL3) = 0 \quad (11)$$

$$D(V_{dc} + VC1) + (1 - D)(V_s - VL2 - VC2) = 0 \quad (12)$$

$$VL2 = nVL3 \quad (13)$$

$$VC1 = \frac{(1 + n)D}{1 - D} VC2 \quad (14)$$

$$VC1 = \frac{(1 + n)D}{[1 - (2 + n)D]} V_s \quad (15)$$

$$VC2 = \frac{1 - D}{[1 - (2 + n)D]} V_s \quad (16)$$

The DC link voltage is

$$V_{pn} = \frac{1}{[1 - (2 + n)D]} V_s = KV_s \quad (17)$$

The boost ratio K is obtainable,

$$K = \frac{1}{[1 - (2 + n)D]} \quad (18)$$

The voltage gain G is obtainable,

$$G = MK = \frac{M}{[1 - (2 + n)D]} \quad (19)$$

where Mis the modulation index.

From the beyond study, the voltage gain of the trans-QZSI is not just coupled with the shoot-through duty cycle D, but also with the turn ratio n of the pairing inductors, as well as the modulation index M of the inverter.

2.2 SPACE VECTOR PULSE WIDTH MODULATION

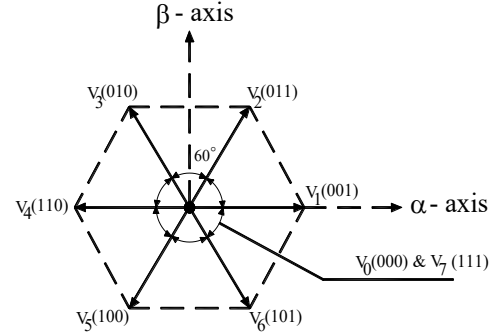


Fig. 5 - Vector diagram.

Since the beyond the diagrams Figs. 5 and Fig. 6, we know V_s is in the 1st sector. V_s is the calculation of two vectors,

$$\vec{V}_a + \vec{V}_b = \vec{V}_s \quad (20)$$

where

\vec{V}_a is the vector along the space vector V_1

\vec{V}_b is the vector along the space vector V_2

One knows V_a is a section of V_1 . V_b is a section of V_2 . If V_1 is tuned ON for T_a times V_a can be roughly. Correspondingly V_2 is tuned ON for T_b times so that V_b is roughly.

$$\vec{V}_a = T_a * \vec{V}_1 \quad (21)$$

$$\vec{v}_b = T_b * \vec{v}_2 \quad (22)$$

$$\vec{v}_s = T_a * \vec{v}_1 + T_b * \vec{v}_2 \quad (23)$$

This way that V_1 is kept back on for T_a period and V_2 is kept back on for T_b period to combine $V_s = T_a + T_b \leq T_{PWM}$. If null vectors are supplementary for T_0 period,

$$T_a + T_b + T_0 = TPWM \quad (24)$$

Hence T_0 is added to keep the zero vectors ON for T_0 period, so that will be equal to $T_a + T_b + T_0$. Now

$$\vec{v}_s * TPWM = T_a * \vec{v}_1 + T_b * \vec{v}_2 + T_0 * (\vec{v}_0 \text{ or } \vec{v}_7) \quad (25)$$

The neighbouring vectors also yield corresponding V_s in other divisions. For an adequately high frequency, the reference vector V_s can be held stable through one switching period (one PWM period) TPWM. Since the vectors V_1 and V_2 are stable, we can associate the TPWM time of the reference vector to the space voltage vectors as

$$\vec{v}_s * TPWM = T_a * V_1 + T_b * V_2 + T_0 * (V_0 \text{ or } V_7) \quad (26)$$

The switching sequence is referred to in Table 1.

Table 1
Switching sequence.

Space Voltage Vectors	Switching States
V0	000
V1	001
V2	011
V3	010
V4	110
V5	100
V6	101
V7	111

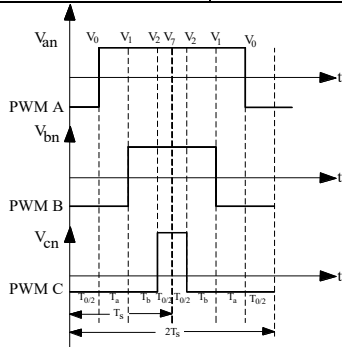


Fig. 6 – Switching state sector I.

3. RESULTS AND DISCUSSION

3.1 SIMULATION RESULT AND DISCUSSION

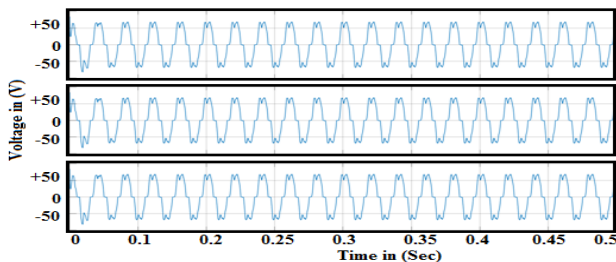


Fig. 7- PMSG output voltage.

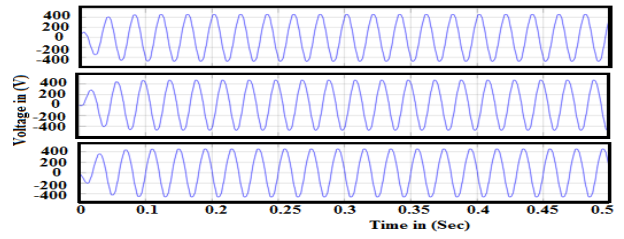


Fig. 8 – Rectifier output voltage.

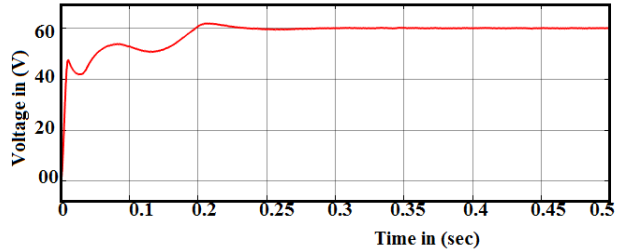


Fig. 9 – Z-source network output.

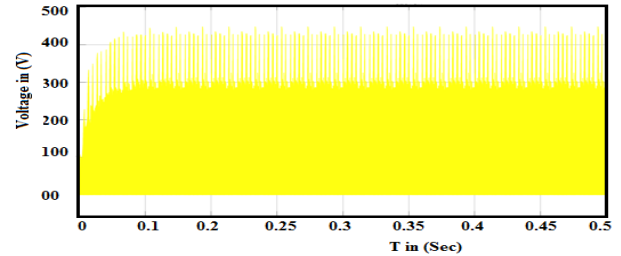


Fig.10 – Inverter output voltage waveform.

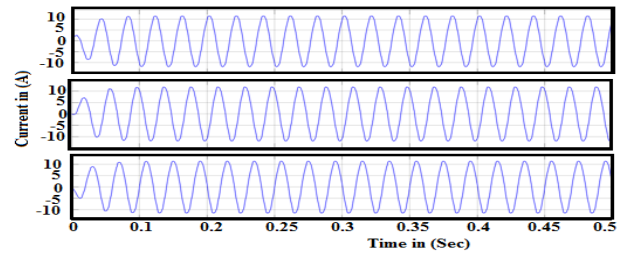


Fig. 11 – Inverter output current waveform.

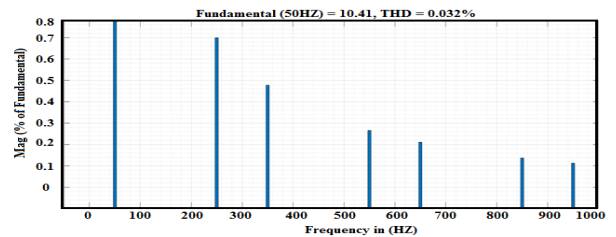


Fig. 12 – Total harmonic distortion.

Initially, the wind turbine rotated at a speed of 15 m/s, at which time PMSG produced 60 V AC, as shown in Fig. 7. PMSG output voltage is fed to a 3-phase diode rectifier circuit. Figure 8 illustrates how this circuit converts 60 AC to almost 60 DC. The shoot-through state is executed via Trans Quasi networks that absorb the DC power. Based on the boost ratio Z source network is boosted up to 420 V as shown in Fig. 9. Further ZSI converts 420 DC to 420 AC voltage and inverter current 12A as shown in Fig. 10 and Fig. 11. Essentially Trans-QZSI output voltage is square wave, using LC filter and sort out the harmonics as well as support of the transformer to provide the pure sine wave

output voltage of the grid side. As seen in Fig. 12, the total harmonic distortion (0.032%) was attained via SVPWM techniques.

3.2 EXPERIMENTAL RESULTS AND DISCUSSION

Figures 13 and 14 show the hardware block diagram and hardware snapshot for the proposed system. Here, 24 V AC is fed to the diode rectifier circuit; this circuit converts the 24 V AC to 24 V DC, as shown in Fig. 15. This 24 V DC is provided to the Z-source network. The Z-source network enhances the input voltage, commonly referred to as the DC rail voltage. Figure 16 illustrates the hardware results of the Z-source network. Due to inductance and capacitance, the voltage has increased (50 V DC). Shoot-through operation is an important one for the boost factor. After using the filter, the Z source network output is almost constant (50V DC), as shown in Fig. 17.

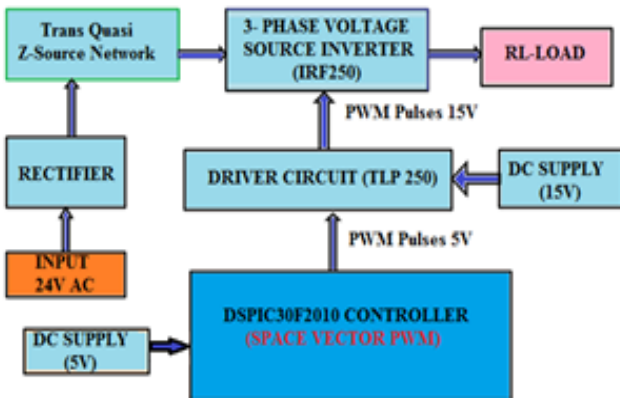


Fig. 13 – Hardware block diagram of proposed system.

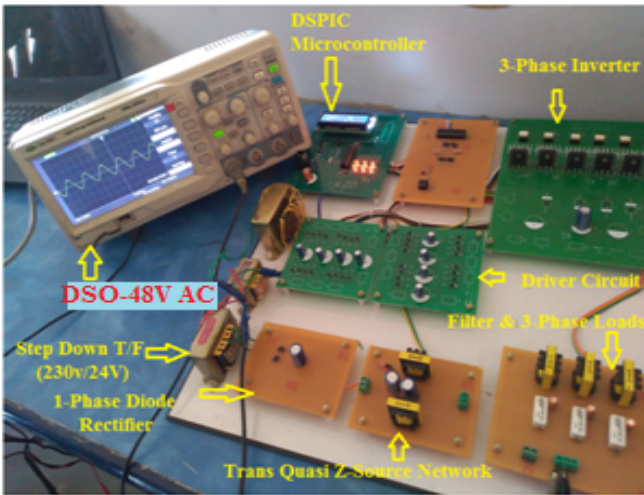


Fig. 14 – Hardware snapshot.



Fig. 15 – Input C voltage (rectifier output) to the Z-source network.

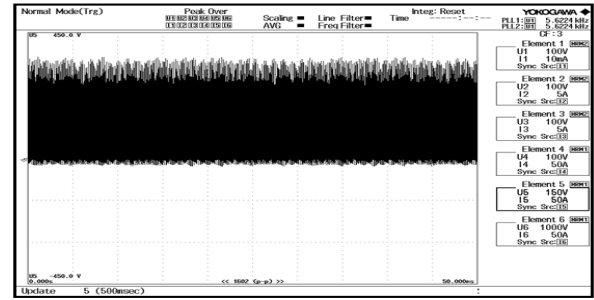


Fig. 16 -Trans quasi-Z-source output DC voltage of the Z-source network.



Fig. 17 – Trans quasi-Z-source output voltage waveform after LC filtering.

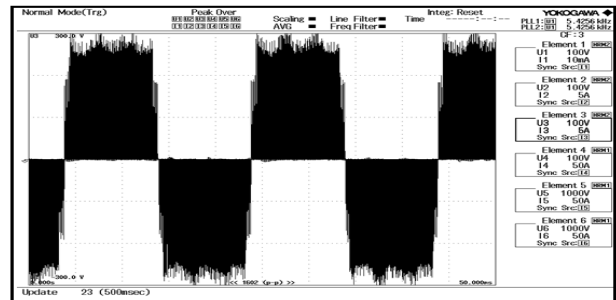


Fig.18 – Trans quasi-Z-source inverter output voltage waveform before LC filtering.

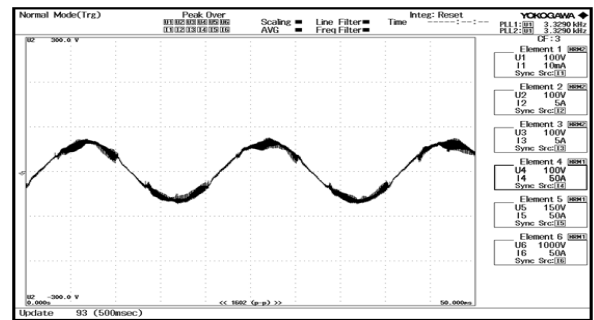


Fig. 19 – Trans QZSI output voltage waveform after LC filtering.



Fig. 20 – Trans-QZSI output voltage THD waveform (2.093%).

The output voltage of the three-phase voltage source inverter (42V AC) using SVPWM technology is displayed in Fig. 18. The shoot-through duty cycle is also included, which avoids over-interruption between two cycles, resulting in lower THD. Now that the LC filter is receiving the phase voltage, the output voltage's harmonics will be reduced (48V AC) as seen in Fig.19. The suggested Z-source network supported 3-phase voltage source inverter's THD waveform displayed in Fig.20. Proposed system complies with the IEEE harmonics standard, as it only deviates by 2.093%.

4. CONCLUSION

This research has simplified the process of connecting the output power to the grid network using the well-established Trans-QZSI. A novel foundation for the space vector PWM technique is presented in this study. The THD level of the proposed simulation model was 0.032% compared to the conventional model [10–19] (Fig. 12). Exciting models with THD values greater than MATLAB/Simulink generates 3%. A voltage of 48V and a reduced total harmonic distortion (THD) of 2.093% are successfully achieved by the prototype hardware configuration (Fig. 12). The simulation's outcomes demonstrate very reasonable output evaluation and state performance. The study looks at the utility of hardware models used in experimental prototypes. The trans-QZSI will be utilized in subsequent assignments to enhance power quality. Since they successfully connected the wind power generated near the electricity board using this novel concept, India and other developing countries have the potential to become a significant source of wind control innovation in the future.

CREDIT AUTHORSHIP CONTRIBUTION

Author_1: Contributed equally to the current study at every level, from problem formulation to results and resolution.

Author_2: Contributed equally to the current study at every level, from problem formulation to results and resolution.

Received on 17 November 2024

REFERENCES

1. J. Zuřňak, V. Kujan, F. Janiĉek, *Simulations and measurements on a self-excited induction generator*, Journal of Electrical Engineering, **69**, 5, pp. 359–365 (2018).
2. A. Subramanian, J. Raman, N. Pachaivannan, *An efficient hybrid converter for D.C.-based renewable energy nanogrid systems*, Rev. Roum. Sci. Techn. – Électrotechn. et Énerg., **66**, 5, pp. 225–230 (2021).
3. O.K. Krinah, R. Lalalou, Z. Ahmida, S. Oudina, *Performance investigation of a wind power system based on double-feed induction generator: Fuzzy versus proportional integral controllers*, Rev. Roum. Sci. Techn. – Électrotechn. et Énerg., **67**, 4, pp. 403–408 (2022).
4. C.M. Nwosu, S.E. Oti, C.U. Ogbuka, *Transient and steady state performance analysis of power flow control in a DFIG variable speed wind turbine*, Journal of Electrical Engineering, **68**, 1, pp. 31–38 (2017).
5. R. Elumalai, *Maximum power quality tracking of A.N.N. controller based DFIG for wind energy conversion system*, Rev. Roum. Sci. Techn. – Électrotechn. et Énerg., **69**, 2, pp. 189–192, Bucarest (2024).
6. V. T. Nguyen, H. V. P. Nguyen, T. B. T. Truong, Q. V. Truong, *A virtual synchronous generator control method in microgrid with vehicle-to-grid system*, Journal of Electrical Engineering, **74**, 6, pp. 492–502 (2023).
7. Z. Boudries, S. Tamalouzt, *Study on sliding mode control of a small size wind turbine permanent magnet synchronous generator system*, Rev. Roum. Sci. Techn. – Électrotechn. et Énerg., Bucarest, **64**, 2, pp. 157–162 (2019).
8. S. Bellarbi, A. Boufertella, *Maximum power wind extraction with feedback linearization control approach*, Rev. Roum. Sci. Techn. – Électrotechn. et Énerg., Bucarest, **67**, 3, pp. 237–240 (2022).
9. D. Babu, R. Bharani Kumar, *Investigation of voltage stability generation of electric power influenced DFIG and PMSG wind energy conversion system*, Electric Power Components and Systems (2023).
10. Y. Tang, S. Xie, C. Zhang, Z. Xu, *Improved Z-source inverter with reduced Z-source capacitor voltage stress and soft-start capability*, IEEE Transactions on Power Electronics, **24**, 2, pp. 409–415 (February 2009).
11. S. Singh, S. Sonar, *Design and analysis of space vector pulse width modulation techniques for Z-source inverter*, International Journal of Power Electronics, **12**, 2, pp. 229 (January 2020).
12. H. Prasad, T. Maity, *Modelling and simulation of trans quasi Z-source inverter as an automatic three-phase power conditioner*, International Journal of Power Electronics (January 2015).
13. S. Bandopadhyay, A. Bandyopadhyay, A. Mondal, *Harmonics reduction and power quality improvement in distributed power flow controller by S.V.P.W.M. and M.G.W.O. technique*, Microsyst Technol, (2024).
14. J.P. Srividhya, K.E. Lakshmi Prabha, S. Jaisiva, C. S.G. Rajan, *Power quality enhancement in smart microgrid system using convolutional neural network integrated with interline power flow controller*, Electr Eng, (2024).
15. P.M. Ansho, M.G. Nisha, *Swarm optimized distributed power flow controller for power quality enhancement in grid-connected hybrid system*, J. Electr. Eng. Technol., **19**, pp. 2047–2057 (2024).
16. R. Anand, G. Devadasu, S. Muthubalaji, *Photovoltaic connected active switched boost quasi-Z-source (A.S.B.-qZ.S.I.)-based multi-level inverter system using Q2OGEO approach*, Environ Sci Pollut Res, **31**, pp. 17164–17181 (2024).
17. J. Sivasubramanian, M.B. Veerayan, *ANN and ANFIS-based control approaches for enhanced performance of solar PV-driven water pumping systems employing quasi Z-source converter*, J. Electr. Eng. Technol., **19**, pp. 3499–3513 (2024).
18. M.K. Thangavel, B.K. Ramasamy, P. Ponnusamy, *Performance analysis of dual space vector modulation technique-based quasi Z-source direct matrix converter*, Electric Power Components and Systems, **48** (2020).
19. J. Dalei, G. Sahu, *An efficient method for feature extraction and selection in power quality recognition*, Electric Power Components and Systems, **50** (2022).
20. A.M. Florez-Tapia, J. Vadillo, A.M. Villate, J.M. Echeverria, *Transient analysis of a trans quasi-Z-source inverter working in discontinuous conduction mode*, Electric Power Systems Research, **151**, pp. 106–114 (2017).